Proc. CIBSE A: Building Serv. Eng. Res. Technol. **18**(1) 17–24 (1997) Printed in Great Britain B378

Summary The paper is the third in a series of four which describe a three-year research project into advanced fabric-energy-storage (FES) systems. It presents the derivation of a theoretical relation for the heat transfer (storage efficiency) within a FES-slab which is used to construct a simple model of the slab. The model is then validated against experimental data and incorporated into the full building simulation, ESP-r. An investigation of the summer time overheating risk in an office equipped with FES-slabs demonstrates the application of the model.

Advanced fabric energy storage III: Theoretical analysis and whole-building simulation

R Winwood†‡ MSc PhD, **R Benstead**† MA MASHRAE and **R Edwards**‡ MSc PhD
†EA Technology, Capenhurst, Chester CH1 6ES, UK
‡University of Manchester Institute of Science and Technology, PO Box 88, Manchester M60 1QD, UK

Received 6 November 1995, in final form 25 June 1996

List of symbols

A Area (m^2)
D... Elemental ...
HTC Heat-transfer coefficient ($W\ m^{-2}K^{-1}$)
l Length (variable) (m)
l' Length of air path (m)
L Height of air path (m)
ME Marginal efficiency
MET Marginal energy-transfer rate (W)
MES Marginal energy-supply rate (W)
q Rate of energy transfer (W)
SE storage efficiency
SHC specific heat capacity ($J\ kg^{-1}K^{-1}$)
St Stanton number
t Time (s)
t' Transit time for air to pass through slab (s)
T Temperature (°C)
U Thermal transmittance ($W\ m^{-2}K^{-1}$)
v Velocity ($m\ s^{-1}$)
V Volume (m^3)
V_{eff} Effective volume (m^3)
δ... Change in ...
Δ... Difference in ...
γ Length (m)
μ Constant
ρ Density ($kg\ m^{-3}$)
ψ Constant

1 Introduction

A previous paper[1] described CFD modelling of the FES-slab under a variety of boundary conditions and defined the parameter 'storage efficiency' (SE), which quantifies the heat transfer between the ventilation air and the slab. This paper shows that, given the slab's average internal heat-transfer coefficient, it is possible to theoretically derive the storage efficiency of any length of slab subjected to any air-flow rate.

2 Theoretical derivation of storage efficiency

A small segment of air is considered as it passes through the slab, as shown in Figure 1. The segment is assumed to be small enough for it to be at a uniform temperature, the concrete's diffusivity is assumed to be large enough to consider the slab to be at a uniform temperature and the slab's thermal capacity is considered to be large enough to consider that, within the length of time for air to pass through the slab, the slab's temperature is constant.

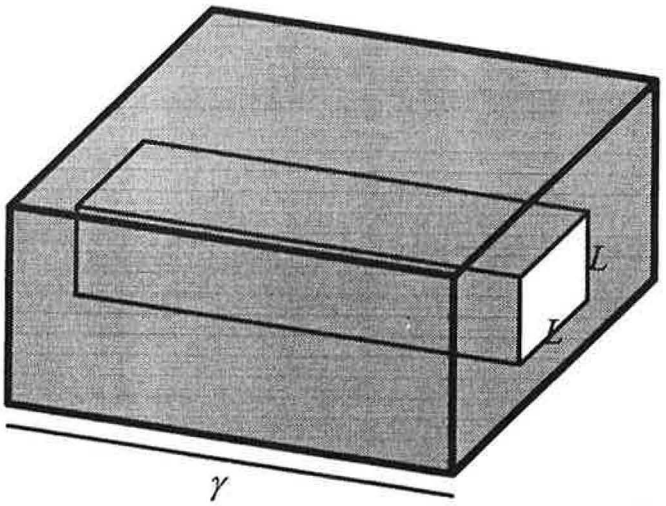

Figure 1 Slab segment considered in theoretical analysis

The rate of energy transfer between the ventilation air and the slab is given by:

$$q(t) = \text{HTC}(t)\ \text{DA}\ \Delta T \tag{1}$$

where ΔT is the temperature difference between the air and the slab, DA is the elemental interface area and HTC is the local heat transfer coefficient.

This heat flow causes the temperature difference ΔT to decay according to

$$\text{d}(\Delta T)/\text{d}t = -q(t)/\text{DV}\ \rho\ \text{SHC} \tag{2}$$

The time-dependent temperature difference between the air and the slab can therefore be evaluated from

$$\Delta T(t) = \Delta T(0) - (\text{DA}/\text{DV}\ \rho\ \text{SHC})\int_0^{t'} (\text{HTC}(t)\ \Delta T(t))\text{d}t \tag{3}$$

If the local heat-transfer coefficient HTC is replaced with an average value $\overline{\text{HTC}}$, equation 3 may be rewritten as

$$\int_0^{t'} \Delta T(t)\text{d}t = (-\text{DV}\ \rho\ \text{SHC}/\text{DA}\ \overline{\text{HTC}})(\Delta T(t) - \Delta T(0)) \tag{4}$$

which is a standard differential equation, the solution of which is:

$$\Delta T(t) = \Delta T(0) \exp-[(DA\overline{HTC}/DV\rho\,SHC)t] \quad (5)$$

Equation 5 may be simplified by substituting

$$DA/DV = 4L\gamma/L^2\gamma = 4/L \quad (6)$$

where L is the length of side of the square core and γ is the length of the volumetric element under consideration. Equation 5 may therefore be rewritten as

$$\Delta T(t) = \Delta T(0) \exp-[(4\overline{HTC}/L\rho\,SHC)t] \quad (7)$$

If t' is defined as the residence time of air within the slab, $\Delta T(0)$ becomes equivalent to the temperature difference between the air and the slab at the inlet and $\Delta T(t')$ is equivalent to the temperature difference as the air leaves the slab. The slab's storage efficiency may therefore be defined theoretically according to

$$SE = 100\% \{1 - \exp-[(4\overline{HTC}/L\rho\,SHC)t']\} \quad (8)$$

Figure 2 compares this theoretical formula with data from CFD models of the slab[1]. The curve labelled 'theory 1' was calculated with an average heat-transfer coefficient of 6.5 W $m^{-2}K^{-1}$, as evaluated from the CFD. The curve labelled 'theory 2' was calculated with the average heat-transfer coefficient evaluated analytically, from the formula[2]

$$\overline{HTC} = St\,SHC\,\rho\,v \quad (9)$$

There is good agreement between the first curve and the CFD results, as expected. The increasing discrepancy at high flow rates is due to the deviation of the local heat-transfer coefficient from its average value as more turbulence is generated at corners in the air path. The second curve accounted for this fact explicitly, as the Stanton number St is a function of the air-flow rate. The curve therefore shows an improved representation of the form of the CFD data at high flow rates, although it is displaced by about 20% along the majority of the curve due to the corners in the airpath, which equation 9 does not account for.

2.1 *Varying slab lengths*

Figure 3 puts equation 8 to use by predicting the storage efficiency of the FES-slab and the generic slab over a range of lengths (where the generic slab's average heat-transfer coefficient was evaluated from CFD data as 4.4 W $m^{-2}K^{-1}$). The figure clearly shows the FES-slab's diminishing advantage; the difference in storage efficiency between 12 m slabs is less than 2%, while the difference between 16 m slabs would be less than 1%.

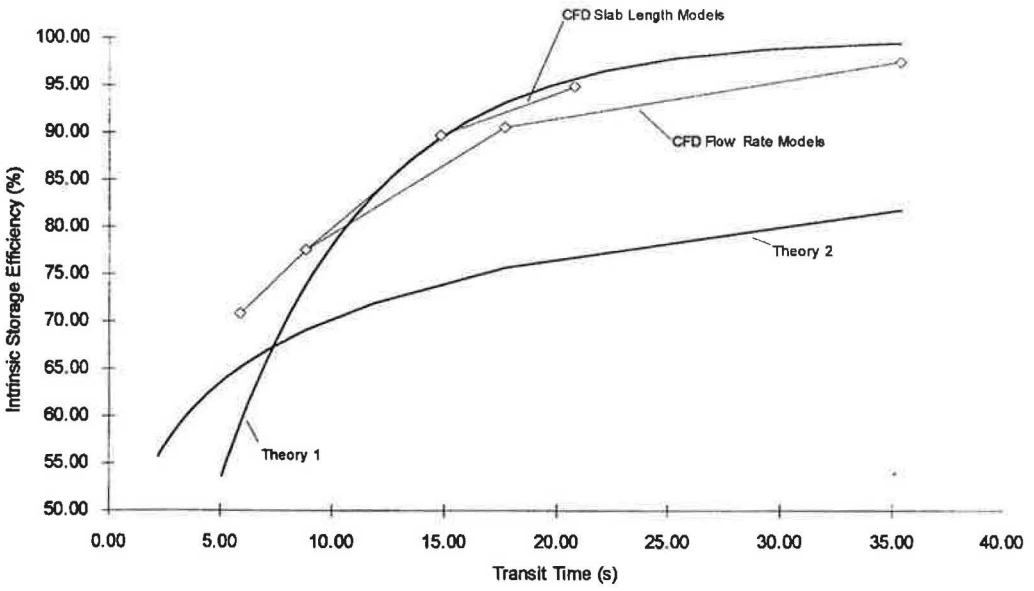

Figure 2 Comparison of experimental and CFD storage efficiencies with theoretical formulae

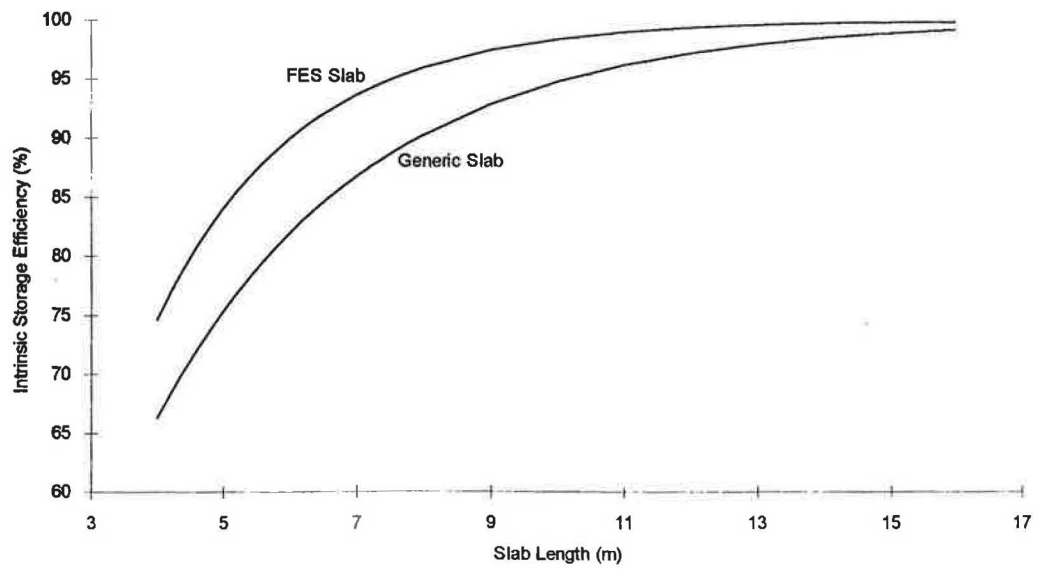

Figure 3 Intrinsic storage efficiency against slab length for a 20 l s^{-1} air flow

2.2 Switchflow

The high storage efficiency of longer slabs has implications for the switchflow system[1]. Equation 8 was used to show that a 12 m slab using switchflow would still have a storage efficiency of around 81%; only 19% less than when the slab uses the 3-core air path.

3 Theoretical derivation of marginal efficiency

The theoretical derivation of storage efficiency was put to further use by investigating the benefit gained from increasing the flow rate through a FES-slab. Figure 4 presents the results for 4 m, 10 m and 16 m slabs. The figure indicates that the transit time for air to pass through the 4 m slab soon became so short that the benefit of increased air flow was virtually eliminated by the reduction in storage efficiency. The longer air paths within the other slabs meant that reasonable transit times were maintained at greater flow rates, making the storage efficiencies less volatile. This indicates that there is very little advantage to be gained from increasing the flow rate beyond a critical value, which is determined by the transit time for air to pass through the slab.

Further investigation showed that it was possible to evaluate the critical flow rate analytically, from the slab's marginal efficiency (the proportion of additional energy which is transferred to the slab). The marginal efficiency was defined according to the following analysis.

The rate of energy supplied to the slab is given by:

$$\text{Rate of energy supply} = \rho \, \text{SHC} \, (T_{in} - T_{slab}) V' \quad (10)$$

which can be rewritten in terms of the transit time for air to pass through the slab:

$$\text{Rate of energy supply} = \rho \, \text{SHC} \, (T_{in} - T_{slab}) l' A'/t' \quad (11)$$

where l' is the length of the air path and A' is its mean cross-sectional area.

The energy which is actually transferred to the slab is therefore found from

$$\text{Rate of energy transfer} = \rho \, \text{SHC} \, (T_{in} - T_{slab}) l' A' \text{SE}(t')/t' \quad (12)$$

where the storage efficiency is given by equation 8.

Thus, simplifying equations 11 and 12 according to equations 13 and 14:

$$\psi = \rho \, \text{SHC} \, (T_{in} - T_{slab}) l' A' \quad (13)$$

$$\mu = 4\overline{\text{HTC}}/L\rho \, \text{SHC} \quad (14)$$

It is possible to express the rates of energy supply and transfer according to equations 15 and 16:

$$\text{Rate of energy supply} = \psi/t' \quad (15)$$

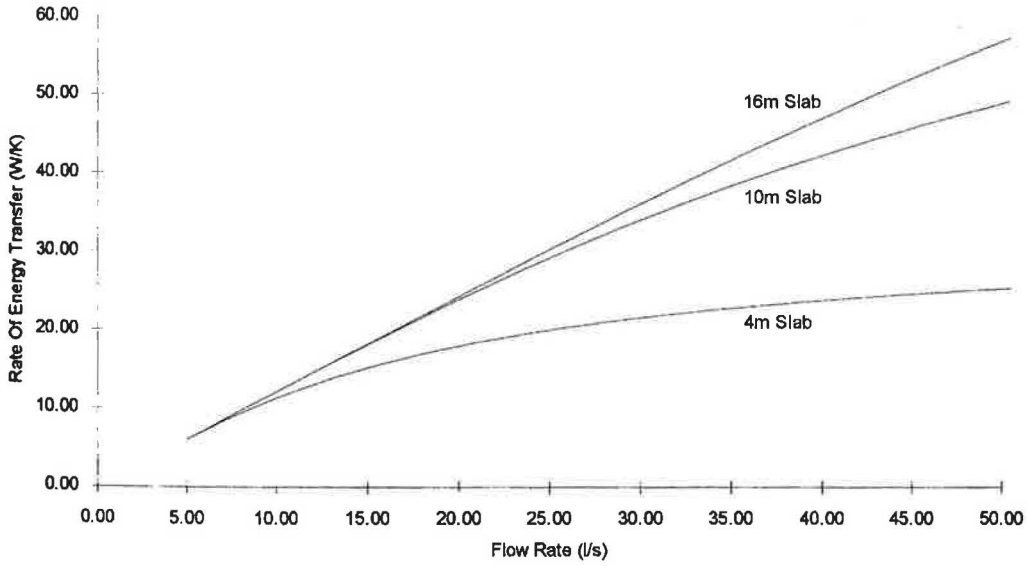

Figure 4 Rate of energy transfer against flow rate

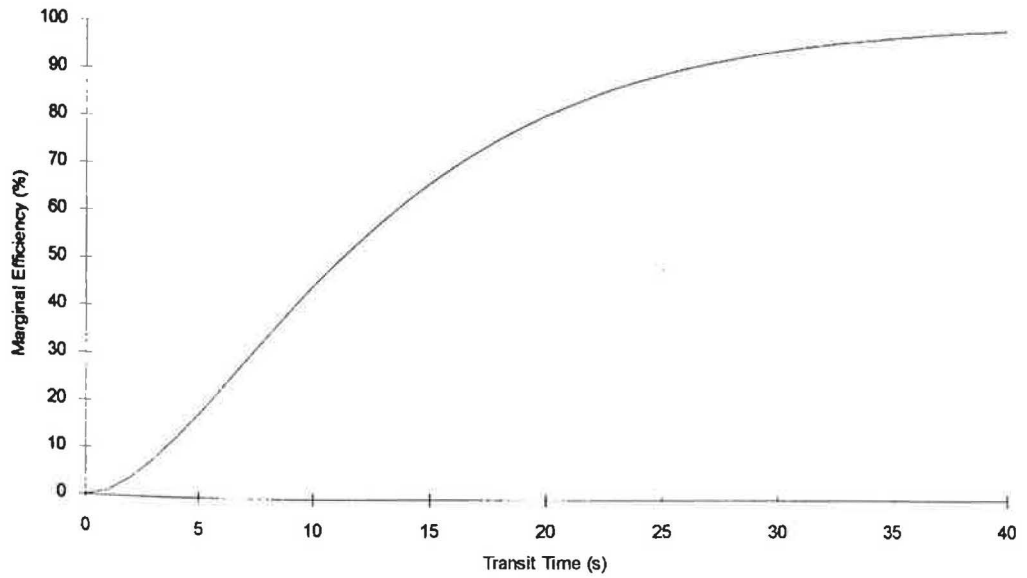

Figure 5 Marginal efficiency of energy transfer against transit time

$$\text{Rate of energy transfer} = (\psi/t')(1 - \exp(-\mu t')) \quad (16)$$

The differentiation of these equations with respect to the transit time for air to pass through the slab yields the marginal energy supply (MES) and the marginal energy transfer (MET), as

$$\text{MES} = -\psi/t'^2 \quad (17)$$

$$\text{MES} = (\psi/t'^2)[(1 + \mu t')\exp(-\mu t') - 1] \quad (18)$$

The marginal efficiency (ME) of a change in the flow rate can therefore be defined as the proportion of the extra energy supplied which is transferred to the slab, according to equation 19:

$$\text{ME} = 100\% \text{ MET/MES} \quad (19)$$

i.e.

$$\text{ME} = 100\% \{1 - [1 + (4\overline{\text{HTC}}/L\rho \text{ SHC})t'] \times \exp-[(4\overline{\text{HTC}}/L\rho \text{ SHC})t']\} \quad (20)$$

Equation 20 is evaluated in Figure 5, which provides the opportunity to calculate the minimum acceptable transit time for any definition of minimum acceptable marginal efficiency. The figure can be used to show that, for example, the transit time for air to pass through a slab cannot be reduced below 10 s without reducing the marginal efficiency below 50% or, in other words, if the flow rate through a 4 m slab is increased from 17 l s^{-1} (transit time ≈ 10 s) to 18 l s^{-1} then less than half of the additional energy will be transferred to the slab.

4 Construction and validation of a multi-node FES-slab model

The preceding section of this paper has dealt with theoretical analysis of results from a CFD model of a single FES-slab, in isolation from other building elements. Subsequent sections describe a simplified model which can be used as part of a full building simulation. This 'multi-node' model was validated on a spreadsheet before being incorporated into an office model constructed within the University of Strathclyde's building simulation program ESP-r.

4.1 Construction

Figure 6 shows the construction of the multi-node model whereby each homogenous layer contained two equally spaced nodes. The model was defined to represent the 4 m FES-slab discussed in the bulk of this research project.

4.2 Heat transfer

Heat exchange at the external surfaces was calculated according to equations 21 and 22, where the U-values were derived from first principles upon the basis of a 5°C temperature difference across the surface:

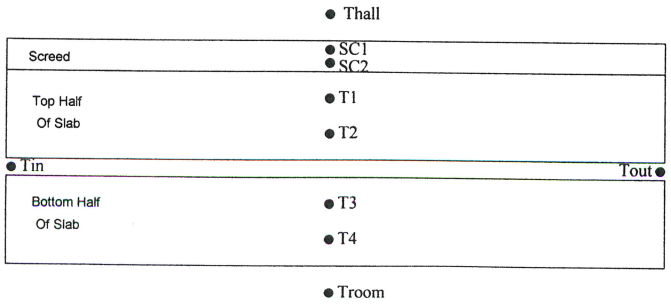

Figure 6 Format of the multi-node model

$$\text{External heat transfer (top surface)} = AU_{top}(T_{hall} - T_{slab})\delta t \quad (21)$$

$$\text{External heat transfer (bottom surface)} = AU_{bot}(T_{room} - T_{slab})\delta t \quad (22)$$

Internal heat transfer between adjacent nodes was also modelled according to the appropriate U-values, while the interaction between the slab and the ventilation air was modelled according to the intrinsic storage efficiency. This reduces the knowledge required by a potential designer to a single parameter, which can be evaluated from equation 8.

4.3 Validation

The model was validated against 11½ days of data from one the bre's experiments[3], as shown in Figures 7 and 8. Table 1 shows that the average disagreement between the model and the experiment was less than 3% over the 11½ days for both the outlet air temperature and the slab bulk temperature (where the simulated slab bulk temperature was approximated to the average of nodes T2 and T3, as shown in Figure 6).

Table 1 Goodness of fit of the multi-node validation

Average disagreement in T_{slab} (%)	Average disagreement in T_{out} (%)
2.4 ± 0.2	1.6 ± 0.1

5 Incorporation of the multi-node model into ESP-r

The multi-node model of an FES-slab was included in the simulation of an office, which was intended to be similar to the Building Research Establishment's FES-slab test cell. The office had dimensions of 4.8 × 4 × 2 m and was covered by four 1.2 × 4 × 0.27 m slabs which, in turn, were covered by a 3.5 cm screed, as shown in Figure 9. The two central slabs were simulated to be active, while the outer slabs were passive. A window of dimensions 1.8 × 1.0 m was positioned in the centre of the exterior wall which, unless otherwise stated, faced south.

Table 2 describes the construction elements used in the model. Interior layers are listed first.

5.1 Boundary conditions

Heat transfer was calculated according to ESP-r defaults, except for the exchange within the slab which, as described above, was calculated on the basis of intrinsic storage efficiency.

The office's interior walls were defined with cyclic boundaries to simulate the presence of identical rooms on three sides. The top and bottom of the model were both defined as adiabatic, preventing vertical heat flow. This mimicked the thermal barrier likely to be presented by a raised floor.

Airflow was simulated with a mass-flow network, as shown in Figure 10. This provided enhanced model definition since it allowed a separate control algorithm to be defined for the fan operation.

Air flow was simulated at a rate of 20 l s^{-1} per active slab, corresponding to an air-change rate of 3.75 ac h^{-1} in the office. The fans were simulated to be operational from 0800 to 1800 h during the week, while at all other times they were thermostatically controlled to operate whenever the room temperature was above 19°C.

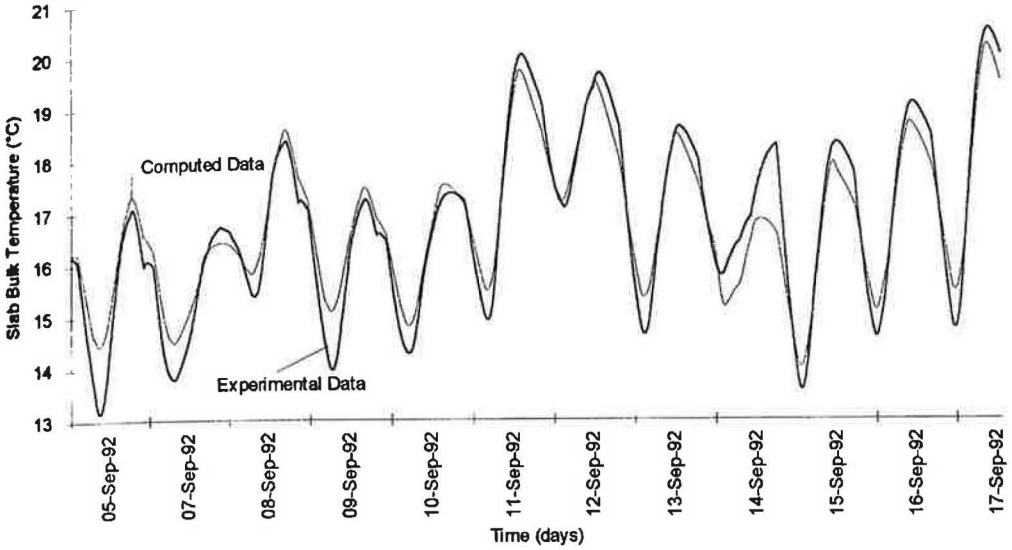

Figure 7 Slab bulk temperatures during the validation of the multi-node model

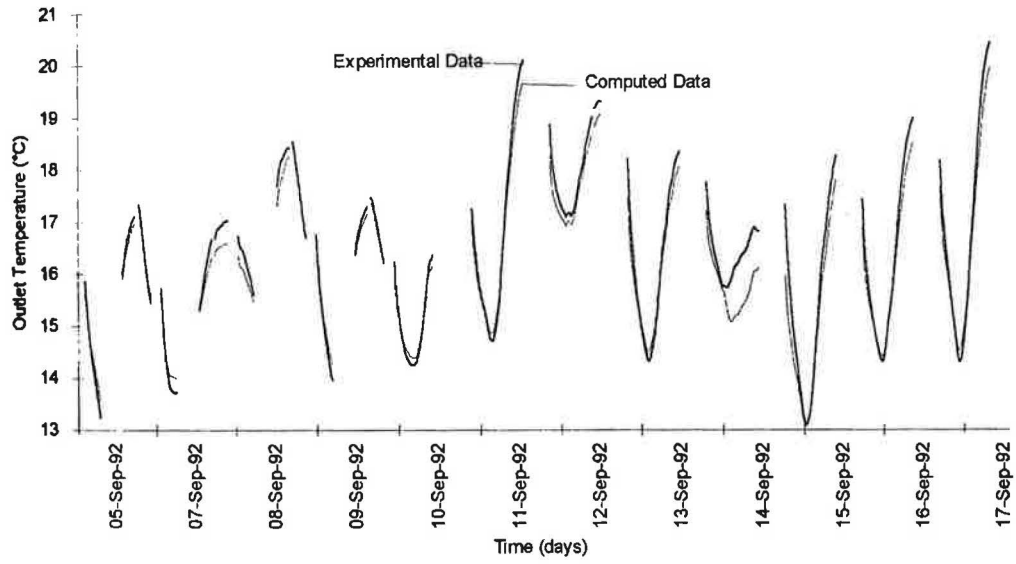

Figure 8 Outlet temperatures during the validation of the multi-node model (gaps represent periods when fans were inoperational)

Unless otherwise stated, heat loads due to occupancy, lighting and information technology equipment were simulated as 30 W m^{-2} from 0800 to 1800 h during the week. The loads were defined to be purely sensible, with a 70:30 split between convective and radiative heat.

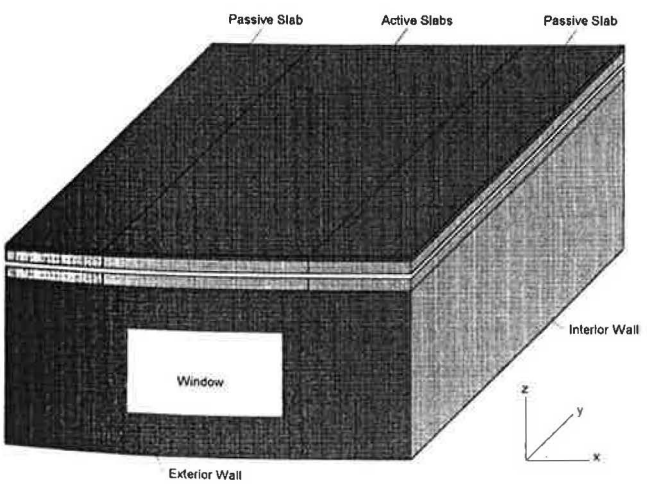

Figure 9 Form of the ESP-r model

The simulations were performed with the default ESP-r weather year; 'CLM67', which is 'indicative of the climate of southern England'.

6 Simulations with ESP-r

The simulations investigated the office's overheating risk with respect to variation of its orientation, heat loads, flow rates and the number of active slabs. They included a two-day 'start-up' period, as suggested by ESP-r, before modelling the office's performance through the three hottest months of the year (June, July and August).

6.1 Results

To permit easy comparison, results are presented in the same format as those produced from the BSRIA's study[4]; a series of graphs showing the number of hours that the room temperature was above a given value.

A short analysis showed that reducing the time step of the model produced a negligible effect upon its results. All of the following analyses were therefore calculated with the default 1 h time interval.

Figure 11 shows that varying the office's orientation had a considerable effect on the peak temperatures experienced

Table 2 Multi-layered building elements within the model

Element	Layer 1	Layer 2	Layer 3	Layer 4	*U*-value (W m^{-2}K^{-1})
Exterior wall	2 cm light plaster	12 cm inner brick	10 cm glass fibre	12 cm outer brick	0.32
Interior walls	2 cm light plaster	12 cm inner brick	2 cm light plaster		1.61
FES-slab bottom	2 cm light plaster	8.2 cm dense concrete			2.89
FES-slab top	8.2 cm dense concrete	3.5 cm screed			3.19
FES-slab end	1 mm precast concrete				5.6
Carpet	1 cm Wilton carpet				2.90
FES-slab end	1 mm precast concrete				5.6
Window	6 mm double-glazed clear glass				2.8

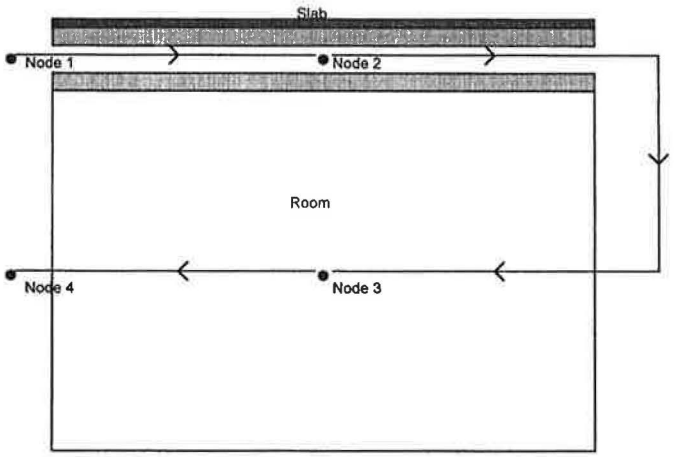

Figure 10 Mass-flow network used to simulate air flow

within the space. This was to be borne out by experimental monitoring of a real building, described in a following paper. The figure also shows that two active slabs were not really sufficient to cool this office.

Figure 12 shows that each 10 W m^{-2} of heat load within the space raised peak internal temperatures by about 2°C.

Figure 13 shows the diminishing benefit of increasing the air-flow rate. In a real building this would be compounded by the sharp increase in fan power at higher ventilation rates.

Figure 14 shows that using all four ceiling slabs reduced peak summer temperatures by at least 2°C. The models investigated the effect of using all four slabs while maintaining the air-change rate in the office (halving the flow through each slab) and while maintaining the flow through each slab (doubling the air-change rate in the office).

Finally, Figure 15 shows that the slab's stable radiant temperature kept peak dry resultant temperatures approximately 0.5°C below the peak dry-bulb temperatures.

7 Discussion and recommendations

7.1 Theoretical analysis

It has been shown theoretically that, if an FES-slab building is to be specified with multi-speed fans as recommended in an earlier paper[1], their maximum and minimum flow rates should be specified to correspond with transit times of 10 s and 35 s.

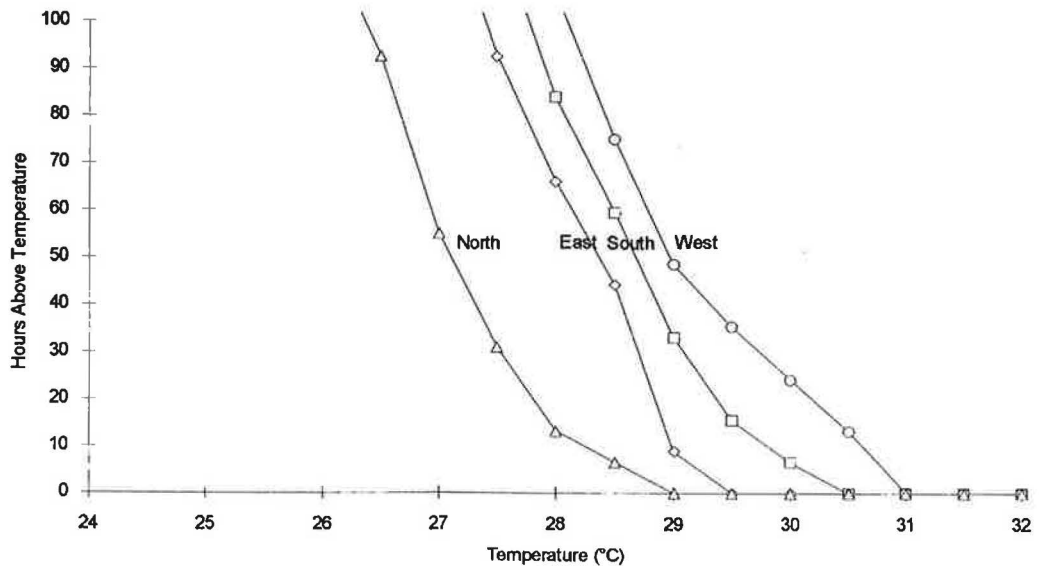

Figure 11 Effect of varying orientation

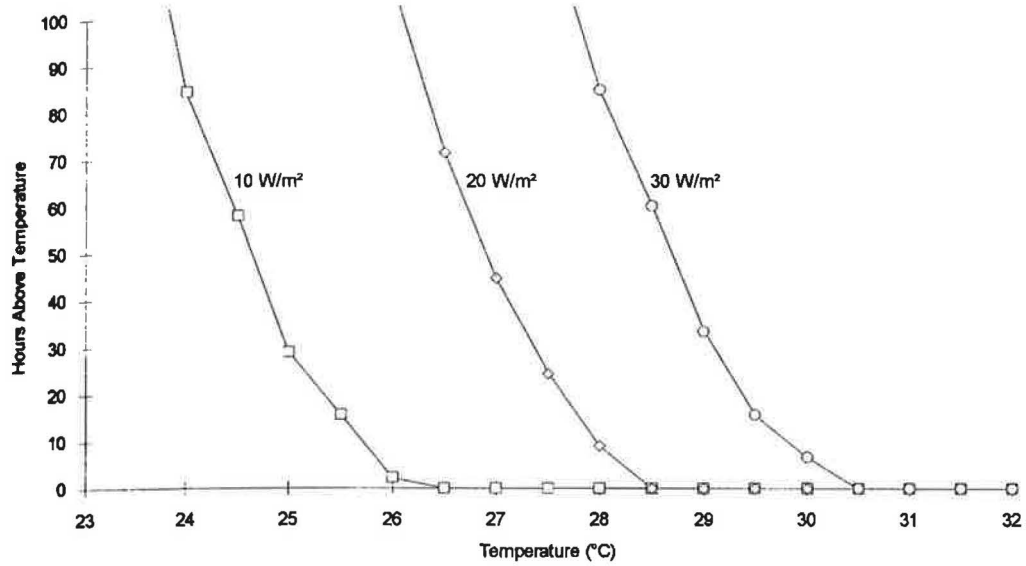

Figure 12 Effect of increasing the heat load within the space

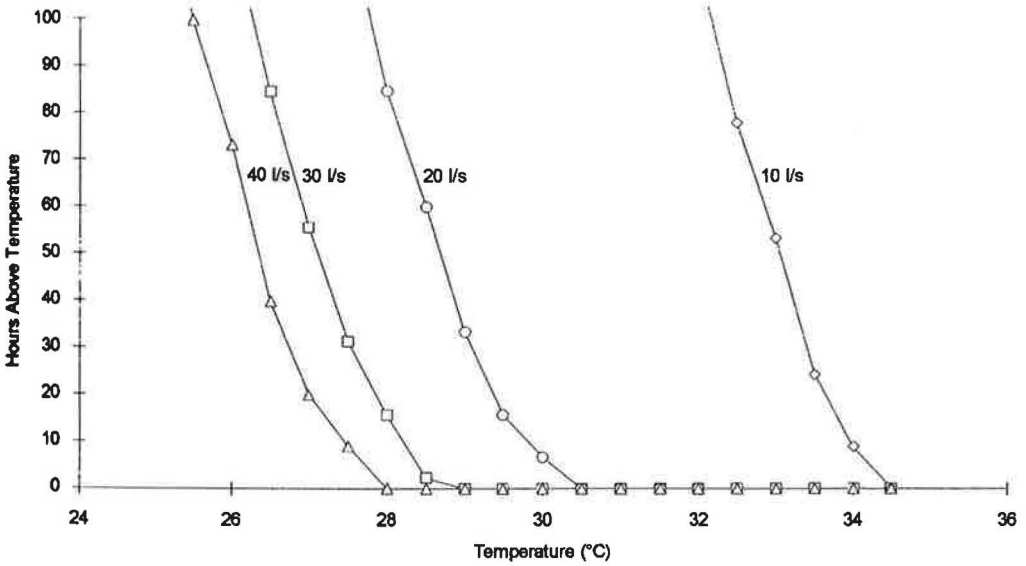

Figure 13 Effect of varying the air-flow rate

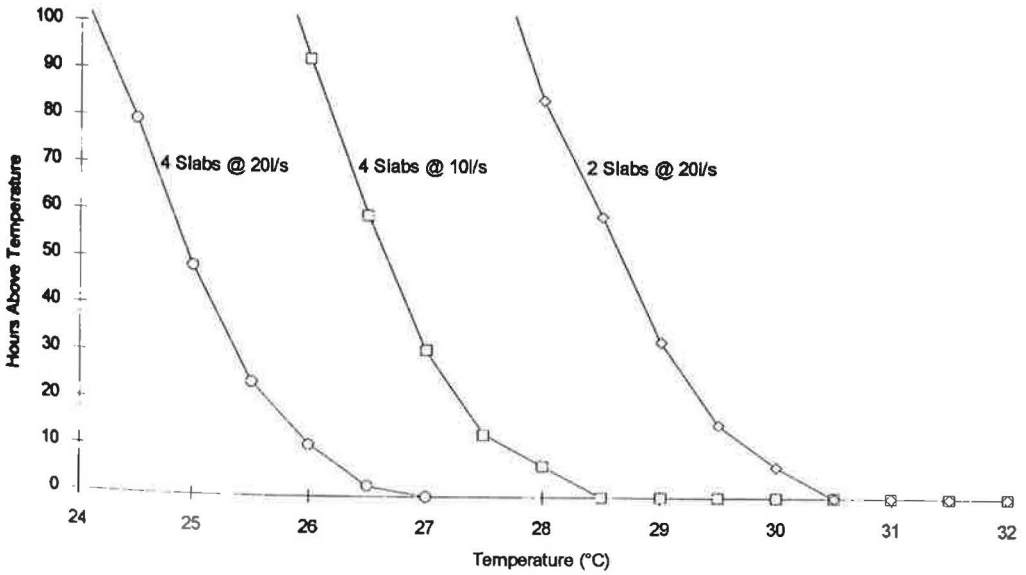

Figure 14 Effect of increasing the number of active nodes

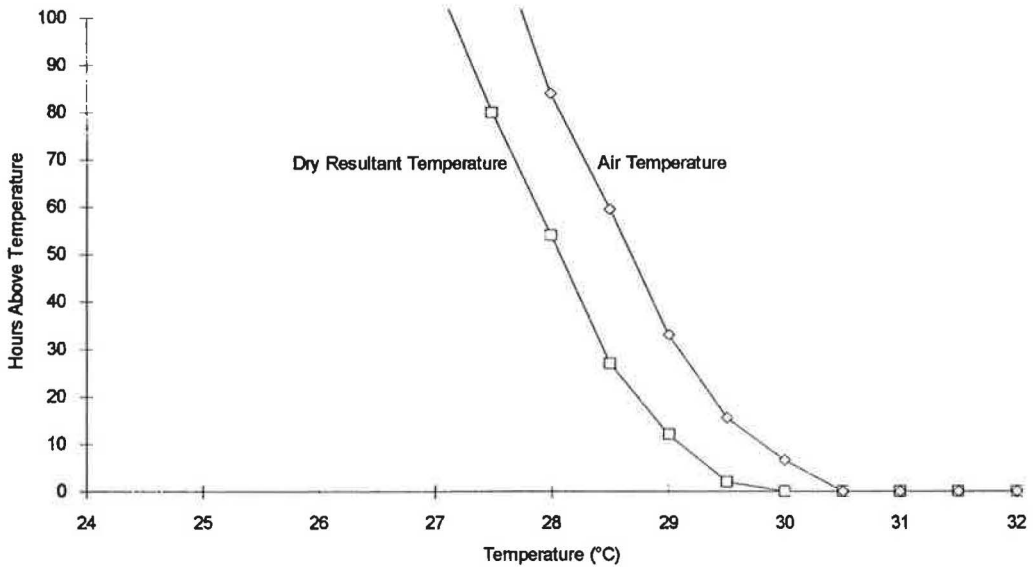

Figure 15 Comparison of peak resultant and dry-bulb temperatures

The theoretical investigation has also shown that, at realistic slab lengths, the storage efficiencies of both the FES-slab and the generic slab are likely to be near to 100%, indicating that the difference in the systems' effectiveness is likely to be more dependent on their effective volume (thermal capacity) than storage efficiency.

7.2 *Multi-node model*

A multi-node model has been constructed and shown to be capable of reproducing the slab's behaviour accurately; however it has the following shortcoming.

Energy exchange is simulated to occur evenly across the internal surfaces, rather than being concentrated in the active central region. The model will therefore be less accurate when simulating advanced FES systems in which the ventilation only interacts with a small portion of the slab, such as a FES-slab using switchflow.

7.3 *ESP-r modelling*

The incorporation of the multi-node model into ESP-r represents the first opportunity to accurately simulate an advanced FES-slab of any length, with any flow rate in a full building model.

Although the ESP-r model was only used to investigate summer time overheating, there is no reason why it could not be modified to simulate winter operation. This investigation was not performed as, bearing in mind that the FES-slab originates from Sweden, there is little doubt that, with appropriately sized heaters, it should be able to cope with British winters.

The ESP-r modelling has highlighted the importance of appropriately distributing heat loads within a building. Consideration of Figure 11 in conjunction with Figure 12 shows that a north-facing office can be expected to sustain about 10 W m^{-2} of extra heat load for the same overheating risk as an equivalent south-facing office.

The results presented in Figures 13 and 14 also imply that, in dealing with high heat loads, it is more effective to increase the amount of active thermal mass than to increase the air-flow rate. This supports an earlier study[1] which showed that the performance of an individual slab was enhanced when its effective volume was maximised. It suggests design implications for offices where the required air-flow rate could be met with only a proportion of the available slabs.

Acknowledgements

This study was funded by a consortium of East Midlands Electricity, Manweb, National Power, Norweb, Scottish Hydro Electric, Scottish Power, South Western Electricity and Yorkshire Electricity under EA Technology's Sponsored Research Programme. The author gratefully acknowledges the sponsors' permission to publish this paper. The author was in receipt of a Postgraduate Training Partnership Award.

References

1 Winwood R B, Benstead R and Edwards R Advanced fabric energy storage II: Computational fluid dynamics modelling *Proc. CIBSE A: Building Serv. Eng. Res. Technol.* 18(1) 7–16 (1996)

2 Rogers and Mayhew *Engineering thermodynamics work and heat transfer* 2nd edn (London: Longman) (1967)

3 Willis S and Wilkins J Mass appeal *Building Serv.: CIBSE J.* **15(3)** 25–27 (1993)

4 Barnard N *Dynamic energy storage in the building fabric* BSRIA Technical Report **TR 9/94** (Bracknell: Building Services Research & Information Association) (1994)